



Measurement of branching fraction of $B_s^0 \rightarrow J/\psi f_0(980)$ decay at CDF

The CDF Collaboration
URL <http://www-cdf.fnal.gov>
(Dated: March 11, 2011)

We present the observation of the decay $B_s^0 \rightarrow J/\psi f_0(980)$ with $f_0(980) \rightarrow \pi^+\pi^-$. Using data collected by the CDF II detector which corresponds to an integrated luminosity of 3.8 fb^{-1} we observe a signal with a statistical significance of 17.9σ . We measure the ratio of branching fractions relative to $B_s^0 \rightarrow J/\psi\phi$ to be

$$R_{f_0/\phi} = \frac{\mathcal{B}(B_s^0 \rightarrow J/\psi f_0(980))}{\mathcal{B}(B_s^0 \rightarrow J/\psi\phi)} \frac{\mathcal{B}(f_0(980) \rightarrow \pi^+\pi^-)}{\mathcal{B}(\phi \rightarrow K^+K^-)} = 0.292 \pm 0.020(\text{stat}) \pm 0.017(\text{sys}).$$

Preliminary Results for Winter 2011 Conferences

I. INTRODUCTION

Since the B_s^0 mixing observation in 2006 [1] particle physics community is excited by searches for CP violation in $B_s^0 \rightarrow J/\psi\phi$ decays. The first results which used flavor tagging to separate B_s^0 and \bar{B}_s^0 showed about 1.5σ deviations from the standard model [2, 3]. In the initial measurements of both Tevatron experiments as well as in the subsequent CDF update [4] a possible contribution from the so-called S -wave contribution was neglected. The S -wave component itself can be non-resonant $B_s^0 \rightarrow J/\psi K^+ K^-$ decay or decay $B_s^0 \rightarrow J/\psi f_0(980)$ with $f_0(980) \rightarrow K^+ K^-$. This neglect caused significant discussion which mainly boiled down to the question whether the departure of Tevatron data from the standard model could be due to a bias caused by neglecting the S -wave contribution or whether the effect is genuine. A summary of the discussion can be found in Refs. [5, 6]. It is also suggested that sufficient signal for the decay $B_s^0 \rightarrow J/\psi f_0(980)$ with $f_0(980) \rightarrow \pi^+ \pi^-$ can be used to measure the CP violating phase $\beta_s^{J/\psi\phi}$ without need of angular analysis [7]. All this generated interest in the decay $B_s^0 \rightarrow J/\psi f_0(980)$. Given the large dataset available at the CDF experiment we expect to observe a significant signal for this decay.

Based on the comparison to D_s meson decays Ref. [5] makes prediction for branching fraction of $B_s^0 \rightarrow J/\psi f_0(980)$ decay relative to $B_s^0 \rightarrow J/\psi\phi$ decay to be

$$R_{f_0/\phi} = \frac{\mathcal{B}(B_s^0 \rightarrow J/\psi f_0(980)) \mathcal{B}(f_0(980) \rightarrow \pi^+ \pi^-)}{\mathcal{B}(B_s^0 \rightarrow J/\psi\phi) \mathcal{B}(\phi \rightarrow K^+ K^-)} \approx 0.2. \quad (1)$$

The CLEO experiment made their own estimate which yields $R = 0.42 \pm 0.11$ [8]. There are several theoretical predictions available. Colangelo, De Fazio and Wang use Light Cone Sum Rules to predict at NLO $\mathcal{B}(B_s^0 \rightarrow J/\psi f_0(980)) = (5.3 \pm 3.9) \cdot 10^{-4}$ [9]. In later work [10] the same authors use QCD factorization to predict $\mathcal{B}(B_s^0 \rightarrow J/\psi f_0(980)) = (4.7 \pm 1.9) \cdot 10^{-4}$ using CDSS form-factors [11] and $\mathcal{B}(B_s^0 \rightarrow J/\psi f_0(980)) = (2.0 \pm 0.8) \cdot 10^{-4}$ using form-factors of Zwicky and Ball [12]. O. Leitner et al. again within the framework of QCD factorization give wide range of R between 0.3 and 0.5. With the world average branching fraction for $B_s^0 \rightarrow J/\psi\phi$ decay of $(1.3 \pm 0.4) \cdot 10^{-3}$ and branching fraction of $f_0(980) \rightarrow \pi^+ \pi^-$ in the region between 0.5-0.8 those predictions translate into a wide range of R of about 0.1-0.5.

The first experimental search was performed by Belle experiment [13]. Their preliminary result does not yield a signal and they extract an upper limit on branching fraction of

$$\mathcal{B}(B_s^0 \rightarrow J/\psi f_0(980)) \mathcal{B}(f_0(980) \rightarrow \pi^+ \pi^-) < 1.63 \cdot 10^{-4} \text{ at } 90\% \text{ C.L.} \quad (2)$$

Recently the LHCb experiment reported the first observation of decay $B_s^0 \rightarrow J/\psi f_0(980)$ with a significance of 12.8σ [14] and measures

$$R_{f_0/\phi} = 0.252_{-0.032}^{+0.046} {}_{-0.033}^{+0.027}. \quad (3)$$

Shortly after LHCb result, Belle collaboration announced result of the updated analysis using 121.4 fb^{-1} of $\Upsilon(5S)$ data [15]. They observe a $B_s^0 \rightarrow J/\psi f_0(980)$ signal with significance of 8.4σ and measure

$$\mathcal{B}(B_s^0 \rightarrow J/\psi f_0(980)) \mathcal{B}(f_0(980) \rightarrow \pi^+ \pi^-) = (1.16_{-0.19}^{+0.31} {}_{-0.17}^{+0.15} {}_{-0.18}^{+0.26}) \cdot 10^{-4} \quad (4)$$

where the first uncertainty is statistical, the second systematical and the third one is an uncertainty on the number of produced $B_s^{(*)0} \bar{B}_s^{(*)0}$ pairs.

In this paper we present confirmation of $B_s^0 \rightarrow J/\psi f_0(980)$ decay followed by $f_0(980) \rightarrow \pi^+ \pi^-$ and measurement of its branching fraction relative to the $B_s^0 \rightarrow J/\psi\phi$ decay. We use data collected by the CDF II detector from February 2002 until October 2008 using the dimuon trigger. The data corresponds to an integrated luminosity of $\mathcal{L} \approx 3.8 \text{ fb}^{-1}$.

II. CDF DETECTOR AND TRIGGER

Among the components and capabilities of the CDF II detector [16] the tracking and muon detection systems are most relevant for this analysis. The tracking system lies within a uniform, axial magnetic field of 1.4 T strength. The inner tracking volume up to a radius of 28 cm is filled with 6 – 7 layers of double-sided silicon microstrip detectors [17]. An additional layer of single-sided silicon is mounted directly to the beam-pipe at a radius of 1.5 cm, providing an excellent resolution of the impact parameter d_0 , defined as the distance of closest approach of the track to the interaction point in the transverse plane. The remainder of the tracking volume up to a radius of 137 cm is occupied with an open-cell drift chamber (COT) [18]. It provides up to 96 measurements along the track with about

half of them being axial and other half stereo information. We detect muons in planes of multi-wire drift chambers [19] in the pseudorapidity range $|\eta| \leq 1.0$.

A three-level trigger system is used for the online event selection. The trigger component most important for this analysis are the extremely fast tracker (XFT) [20], which, at the level 1 groups COT hits into tracks in the plane transverse to the beamline. The events are selected by a dimuon trigger [16] which requires two tracks of opposite charge found by the XFT which match to a track segments in the muon chambers and have a dimuon invariant mass from 2.7 to 4.0 GeV/c^2 .

III. RECONSTRUCTION AND CANDIDATE SELECTION

In the offline reconstruction we first combine two muon candidates to a J/ψ candidate. As muon candidates we use all tracks which can be matched to a track segment in the muon detectors. The J/ψ candidate is subject to a kinematical fit with vertex constrain. Afterwards we combine the J/ψ candidate with two other tracks which are assumed to be pions and have an invariant mass between 0.85 and 1.2 GeV/c^2 to form an $B_s^0 \rightarrow J/\psi f_0(980)$ candidate. In the final step a kinematic fit of $B_s^0 \rightarrow J/\psi f_0(980)$ candidate is performed. In this fit we constrain all four tracks to originate from a common vertex and the two muons forming the J/ψ are constrained to have an invariant mass equal to the world average J/ψ mass. In a similar way we also reconstruct $B_s^0 \rightarrow J/\psi \phi$ candidates using pairs of tracks of opposite charge assumed to be kaons and having invariant mass between 1.009 and 1.029 GeV/c^2 . In addition we place a minimal requirement on the track quality, the quality of kinematical fit, the significance of proper decay time of the B_s^0 candidate and the minimum transverse momentum of the B_s^0 candidate. Those aim at removing a large fraction of obvious background and ensuring high quality measurements of properties for each candidate.

The actual selection is performed by a neural network based on the NEUROBAYES package [21, 22]. The neural network combines several input quantities to form a single output quantity on which the selection is performed. The output of the neural network corresponds to a transformation from a multidimensional space of input quantities to a one-dimensional output quantity. The transformation is chosen during a training phase in a way that it maximizes the separation between signal and background. For the training of the neural network we need two sets of events with a known classification of signal or background. The background sample is taken from data using candidates with the $J/\psi \pi^+ \pi^-$ invariant mass between 5.45 and 5.55 GeV/c^2 . As a signal sample we use simulated events. We generate the kinematic distributions of B_s^0 according to the measured b -hadron momentum distribution. The generated B_s^0 particles are decayed using EVTGEN package [23] into the $J/\psi f_0(980)$ final state. After the decay each event is passed through the standard CDF detector simulation, based on the GEANT3 package [24, 25]. The resulting events are reconstructed with the same reconstruction software as real data events. The inputs to the neural network, ordered by their importance, are: the transverse momentum of $f_0(980)$, the χ^2 of the kinematical fit of B_s^0 candidate using information in the plane transverse to the beamline, the proper decay time of B_s^0 candidate, the quality of the kinematical fit of B_s^0 candidate, the helicity angle of the positive pion, the transverse momentum of B_s^0 candidate, the quality of the kinematical fit of two pions with common vertex constraint, the helicity angle of the positive muon and the quality of the kinematical fit of two muons with common vertex constraint. For the selection of $B_s^0 \rightarrow J/\psi \phi$ decays we use the same neural network without retraining, just exchange $f_0(980)$ quantities by ϕ quantities and pions to kaons.

We select the threshold on the neural network output by maximizing $\epsilon/(2.5 + \sqrt{N_b})$ [26], where ϵ is the reconstruction efficiency for $B_s^0 \rightarrow J/\psi f_0(980)$ decays and N_b is the number of background events estimated from the $J/\psi \pi^+ \pi^-$ mass sideband. The invariant mass distributions of selected $B_s^0 \rightarrow J/\psi f_0(980)$ and $B_s^0 \rightarrow J/\psi \phi$ candidates are shown in Fig. 1. A clear signal at around 5.36 GeV/c^2 is visible in both mass distributions.

We study possible physics backgrounds using simulated events with all b -hadrons produced and decayed inclusively to final states containing J/ψ . While several physics backgrounds appear in the $J/\psi \pi^+ \pi^-$ mass spectrum, none contributes significantly directly under the B_s^0 peak. The most prominent physics backgrounds are $B^0 \rightarrow J/\psi K^{*0}(892)$ with $K^{*0}(892) \rightarrow K\pi$ and $B^0 \rightarrow J/\psi \pi^+ \pi^-$. In the first case the kaon is misreconstructed as a pion and gives rise to a large fraction of the structure seen below 5.22 GeV/c^2 , second one is correctly reconstructed and is responsible for the indication of a peak between the B_s^0 signal and the large structure at lower masses. The stacked histogram of physics backgrounds derived from simulation is shown Fig. 2.

IV. FIT DESCRIPTION

We use an unbinned extended maximum likelihood fit of the invariant mass to extract the number of B_s^0 decays in our samples. In order to simplify the fit, we restrict the fit to mass range from 5.26 GeV/c^2 to 5.5 GeV/c^2 . The

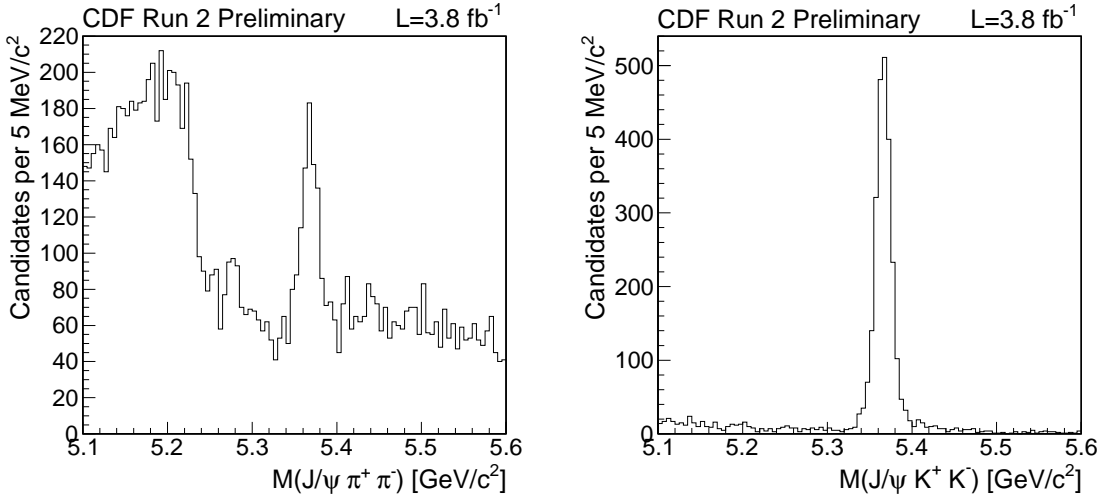


FIG. 1. The invariant mass distribution of selected $B_s^0 \rightarrow J/\psi f_0(980)$ candidates (left) and of $B_s^0 \rightarrow J/\psi \phi$ candidates (right).

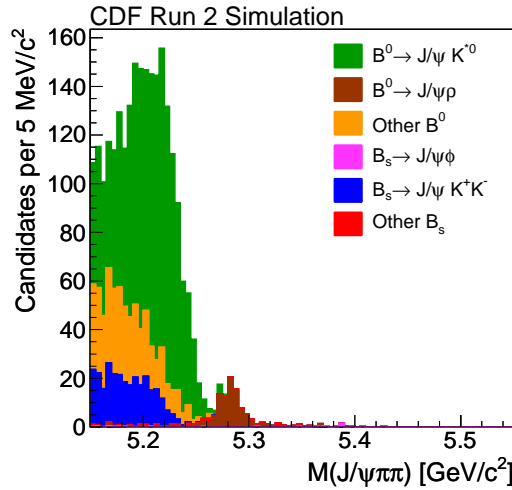


FIG. 2. The stacked histogram of physics backgrounds derived from simulation.

likelihood is written as

$$\mathcal{L} = \prod_{i=1}^N [N_s \cdot P_s(m_i) + N_b \cdot P_b(m_i) + f_{phb} \cdot N_s \cdot P_{phb}(m_i) + N_{B^0} \cdot P_s(m_i)] \cdot e^{-(N_s + N_b + N_s \cdot f_{phb} + N_{B^0})}, \quad (5)$$

where the N is the total number of candidates in the sample, the N_s and N_b are the number of signal and background events, the m_i is the invariant mass of i -th candidate and the $P_x(m_i)$ denotes the probability density functions (PDFs) for different components. The first two terms represent signal and combinatorial background. The other two terms are considered to describe physics motivated backgrounds which we discuss below.

The signal PDF $P_s(m_i)$ is parameterized by a sum of two Gaussian functions with common mean. The fractions between corresponding Gaussian functions and their widths are determined from simulated events. About 82% of the $B_s^0 \rightarrow J/\psi f_0(980)$ decays are contained in a narrower Gaussian with width of about $9.4 \text{ MeV}/c^2$. The broader Gaussian has width of about $18.4 \text{ MeV}/c^2$. In a case of $B_s^0 \rightarrow J/\psi \phi$, narrow Gaussian with width of about $7.2 \text{ MeV}/c^2$ contains about 79% of area with rest of the events having width of $13.3 \text{ MeV}/c^2$. To take into account possible differences between simulation and data we multiply all widths by single scaling parameter t . In the fits all parameters of the PDF are fixed except the position of Gaussians and the scaling parameter t in fit to $J/\psi K^+ K^-$ fit. For the $J/\psi \pi^+ \pi^-$ fit we fix the width scale t and the position of signal to the values determined in fit to $J/\psi K^+ K^-$

candidates. The value of the scaling parameter t is found to be about 1.12 and the position of the signal is consistent with the world average B_s^0 mass [27].

The combinatorial background PDF $P_b(m_i)$ is parameterized using linear function. In both fits we leave its parameter floating. In each of the two fits there is one physics motivated background. In the case of the $J/\psi\pi^+\pi^-$ spectrum it describes properly reconstructed $B^0 \rightarrow J/\psi\pi^+\pi^-$ decays using a shape identical to B_s^0 signal and position fixed to world average B^0 mass [27]. The number of B^0 events N_{B^0} is left free in the fit. For the $J/\psi K^+K^-$ fit we have contribution from $B^0 \rightarrow J/\psi K^{*0}$ decay where the pion from $K^{*0}(892)$ decay is misreconstructed as a kaon. This contribution peaks at mass of about $5.36 \text{ GeV}/c^2$ with an asymmetric tail towards larger masses. The shape itself is parameterized by a sum of Gaussian function and exponential function convolved with a Gaussian. The parameters are derived from simulated $B^0 \rightarrow J/\psi K^{*0}$ events. The absolute normalization of this component is fixed to $(3.04 \pm 0.99) \cdot 10^{-2}$ which is derived from the CDF Run 1 measurement of the ratio of cross section times branching fraction for $B_s^0 \rightarrow J/\psi\phi$ and $B^0 \rightarrow J/\psi K^{*0}$ decays [28], the world average branching fractions for ϕ and $K^{*0}(892)$ [27] and a ratio of reconstruction efficiencies obtained from simulation.

V. EFFICIENCY

In order to extract the ratio of branching fractions we need to estimate the relative efficiency for reconstruction of $B_s^0 \rightarrow J/\psi f_0(980)$ and $B_s^0 \rightarrow J/\psi\phi$ decays $\epsilon_{rel} = \epsilon(B_s^0 \rightarrow J/\psi\phi)/\epsilon(B_s^0 \rightarrow J/\psi f_0(980))$. We estimate it using simulated events in which we generate single B_s^0 meson per event. This is then decayed with equal probabilities to $B_s^0 \rightarrow J/\psi f_0(980)$ or $B_s^0 \rightarrow J/\psi\phi$ final states with exclusive $J/\psi \rightarrow \mu^+\mu^-$, $\phi \rightarrow K^+K^-$ and $f_0(980) \rightarrow \pi^+\pi^-$. Generated events are then processed through detailed detector simulation based on GEANT3 [24, 25] and offline reconstruction software used to reconstruct data. In both cases proper angular and decay time distributions are generated. For the $B_s^0 \rightarrow J/\psi\phi$ decays these are based on the preliminary result of angular distributions analysis [29] which yields values

$$\begin{aligned}\tau &= 458.6 \pm 8.4 \text{ } \mu\text{m}, \\ \Delta\Gamma &= 0.075 \pm 0.036 \text{ ps}^{-1}, \\ |A_0|^2 &= 0.524 \pm 0.020, \\ |A_{||}|^2 &= 0.231 \pm 0.021.\end{aligned}$$

As a strong phase between A_0 and $A_{||}$ is not measured we use the world average value from $B^0 \rightarrow J/\psi K^{*0}$ decays $\phi_{||} = -2.86 \pm 0.11$ [27] as a reasonable approximation [30]. An additional peculiarity of the $B_s^0 \rightarrow J/\psi f_0(980)$ decay is an unusual mass shape of the $f_0(980)$ meson. It is modeled using a Flatté distribution [31] with input parameters measured by the BES experiment [32] to be

$$\begin{aligned}m_0 &= 965 \pm 8 \pm 6 \text{ MeV}/c^2, \\ g_\pi &= 165 \pm 10 \pm 15 \text{ MeV}/c^2, \\ g_K/g_\pi &= 4.21 \pm 0.25 \pm 0.21.\end{aligned}$$

With all those inputs into simulation we find $\epsilon_{rel} = 1.178$.

VI. SYSTEMATIC UNCERTAINTIES

We investigate several sources of systematic uncertainties, which can affect the measured branching fraction. They can be broadly separated into two classes, one dealing with assumptions made in the fits and which affects yields and the other one related to assumptions in the efficiency estimation. In the first class we estimate uncertainties by refitting data with a modified assumption and take the difference with respect to the original value as an uncertainty. For the second class we recalculate the efficiency with a modified assumption and take the difference with respect to the default efficiency as an uncertainty unless specified otherwise. The summary of assigned uncertainties is given in table I.

For the yield of $B_s^0 \rightarrow J/\psi\phi$ we investigate the effect of the assumption on the combinatorial background shape, the limited knowledge of misreconstructed $B^0 \rightarrow J/\psi K^{*0}$ decays and the shape of signal PDF. The uncertainty due to the shape of combinatorial background is estimated by changing from the first order polynomial to a constant or a second order polynomial. For the physics background we vary the normalization of the component in the fit and use an alternative shape determined by varying the momentum distribution and the decay amplitudes of $B^0 \rightarrow J/\psi K^{*0}$ in simulation. Finally to estimate the effect of signal PDF parameterization we use an alternative model with single

| Source | $B_s^0 \rightarrow J/\psi\phi$ | $B_s^0 \rightarrow J/\psi f_0(980)$ | ϵ_{rel} |
|-----------------------|--------------------------------|-------------------------------------|------------------|
| Combinatorial bg. | 34 | 22 | - |
| Physics bg | 13 | - | - |
| Resolution | 32 | 9.8 | - |
| Resolution scale | - | 7.5 | - |
| B_s^0 mass | - | 0.5 | - |
| Yield summary | 49 | 25 | - |
| MC statistics | - | - | 0.012 |
| Momentum distribution | - | - | 0.011 |
| Physics of decays | - | - | 0.033 |
| Trigger paths | - | - | 0.016 |
| Efficiency summary | - | - | 0.040 |

TABLE I. The summary of assigned systematic uncertainties.

Gaussian rather than two Gauss functions and an alternative shape from simulation where we vary the momentum distribution of produced B_s^0 mesons and the decay amplitudes of $B_s^0 \rightarrow J/\psi\phi$ decay.

To estimate the uncertainty on the $B_s^0 \rightarrow J/\psi f_0(980)$ yield we follow procedure for $B_s^0 \rightarrow J/\psi\phi$. For the sensitivity to parameterization of the combinatorial background we switch to a second order polynomial or a constant as alternative parameterizations. For the shape of signal PDF we use two alternatives, one with a single Gaussian function instead of two and another one with two Gaussians, but varying the momentum distribution in simulation. We vary also the position of the $B_s^0 \rightarrow J/\psi f_0(980)$ signal and the resolution scale parameter which are fixed in the $J/\psi\pi^+\pi^-$ fit.

The systematic uncertainty on the relative efficiency stems from the statistics of simulation, an imperfect knowledge of momentum distribution, physics parameters of decays like lifetimes or decay amplitudes and differences in the efficiencies of online selection of events. To estimate the effect of the imperfect knowledge of the momentum distribution we vary the production distribution in simulation. The physics parameters entering the simulation are grouped into three categories, those defining the $f_0(980)$ mass shape, the ones determining decay amplitudes in $B_s^0 \rightarrow J/\psi\phi$ decays and those dealing with the lifetimes of two B_s^0 mass eigenstates. In the first two cases we vary each parameter independently and add all effects in quadrature. For the last case we vary the mean lifetime τ and the decay width difference $\Delta\Gamma$ simultaneously and take the largest variation as uncertainty. We add uncertainty from the third class in quadrature with all others to obtain uncertainty due to the physics of decays. The last effect deals with how events are selected during the data taking. The CDF trigger has several different sets of requirements for selection of events to store for the data analysis. The ones used in this analysis can be broadly sorted into three classes depending on momentum thresholds and which subdetectors detected muons. While this is modeled reasonably well, there is no a priori information whether simulation provides right fraction between three classes. To estimate how large effect this can have we calculate efficiency for each class separately and take half of the largest difference as uncertainty.

To obtain the total uncertainty we add all partial uncertainties in quadrature. In total we assigned 49 events as the systematic uncertainty on $B_s^0 \rightarrow J/\psi\phi$ yield, 25 events on $B_s^0 \rightarrow J/\psi f_0(980)$ yield and 0.040 on relative efficiency ϵ_{rel} .

VII. RESULTS

As a result of the fit we find $571 \pm 37 \pm 25$ $B_s^0 \rightarrow J/\psi f_0(980)$ signal events and $2302 \pm 49 \pm 49$ $B_s^0 \rightarrow J/\psi\phi$ events. In the $J/\psi\pi^+\pi^-$ fit we observe $179 \pm 36(\text{stat})$ B^0 events. The projection of the fit for $B_s^0 \rightarrow J/\psi f_0(980)$ is shown in Fig. 3 together with likelihood profile over number of signal events. Analogous information for the $B_s^0 \rightarrow J/\psi\phi$ fit is shown in Fig. 4. In order to check our interpretation of the signal in $J/\psi\pi^+\pi^-$ distribution being due to the $B_s^0 \rightarrow J/\psi f_0(980)$ decays we show the invariant mass distribution of the pions for pure B_s^0 signal in Fig. 5. To obtain the distribution of pure B_s^0 signal we fit the $J/\psi\pi^+\pi^-$ mass distribution in the range 5.26 to 5.45 GeV/ c^2 for each bin. We fit dipion mass distribution using the Flatté parameterization. The obtained parameters $m_0 = 989.6 \pm 9.9(\text{stat})$ MeV/ c^2 , $g_\pi = 141 \pm 19(\text{stat})$ MeV/ c^2 and $g_K/g_\pi = 2.3 \pm 1.3(\text{stat})$ are in reasonable agreement with the ones measured by the BES collaboration with fit probability of 23.4%. In Figs. 6 and 7 we show the positive muon and pion helicity angle distributions. Those are corrected for the relative efficiencies in different bins and fit using theoretical expectation for $B_s^0 \rightarrow J/\psi f_0(980)$ signal. We use χ^2 test to evaluate the consistency of angular distributions in data with expectation. For distribution of $\cos(\theta_{\mu^+})$ we obtain $\chi^2/ndf = 7.9/20$ which corresponds to 99% probability and for $|\cos(\theta_{\mu^+})|$ we find $\chi^2/ndf = 3.8/10$ corresponding to 96% probability. Similarly for $\cos(\theta_{\pi^+})$ the $\chi^2/ndf = 15/20$ giving 78% probability and $\chi^2/ndf = 10/10$ giving 40% probability for $|\cos(\theta_{\pi^+})|$. Given that the dipion mass as well as the angular distributions are consistent with expectations we interpret our signal as coming solely from the

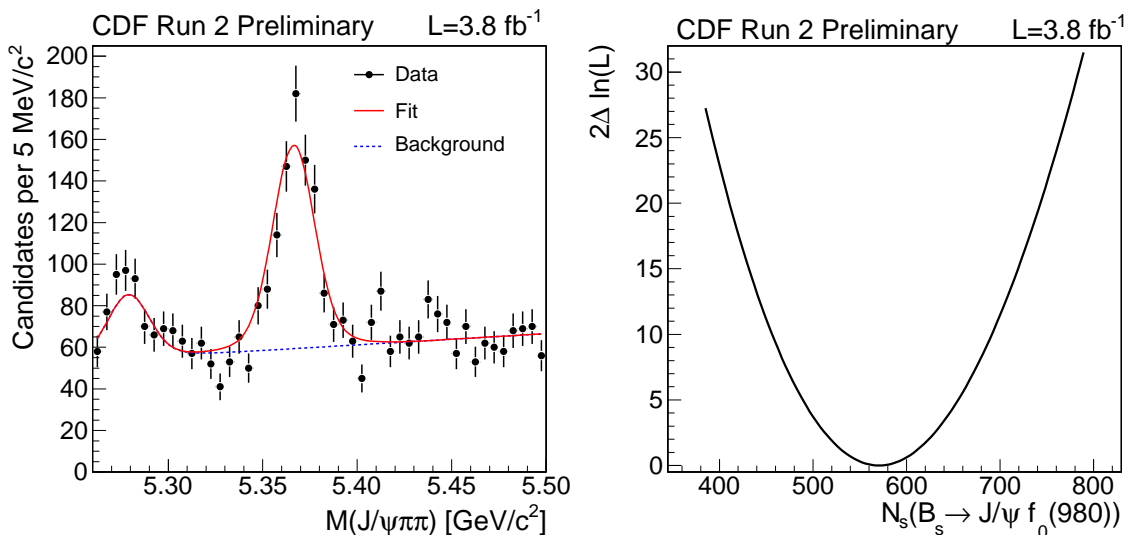


FIG. 3. The projection of the fit of $B_s^0 \rightarrow J/\psi f_0(980)$ decay mode (left) and the likelihood scan over number of signal events (right).

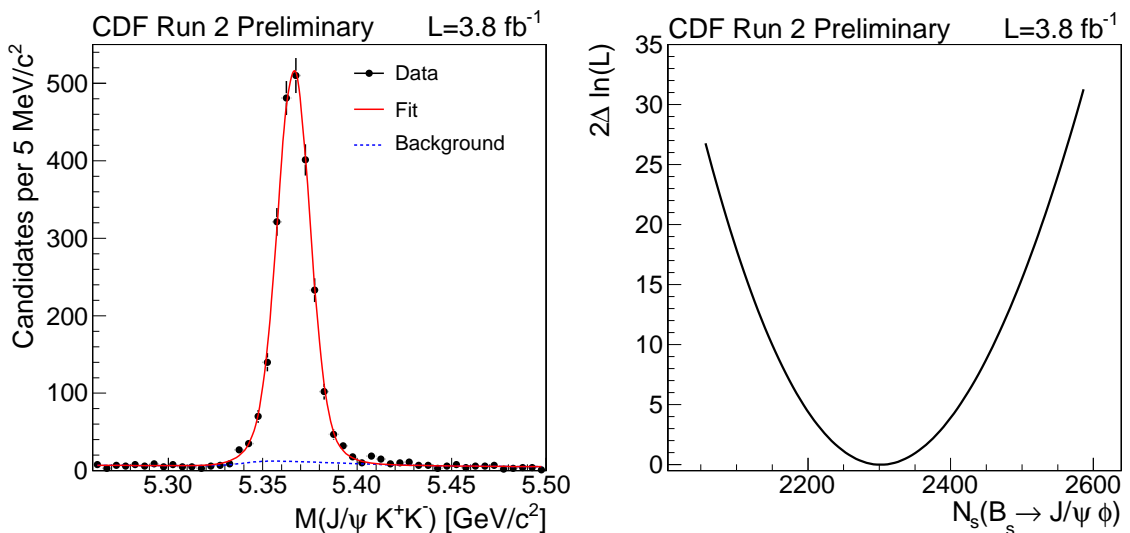


FIG. 4. The projection of the fit of $B_s^0 \rightarrow J/\psi \phi$ decay mode (left) and the likelihood scan over number of signal events (right).

$B_s^0 \rightarrow J/\psi f_0(980)$ decays. On the other hand as our dipion mass window from 0.85 to 1.2 GeV/c^2 is rather large we cannot exclude contribution from other higher mass states to our signal with present statistics. For completeness the statistical significance of $B_s^0 \rightarrow J/\psi f_0(980)$ signal is evaluated using the difference in log-likelihoods between fits with and without signal. The two fits differ by a single parameter being the number of signal events. We obtain the statistical significance of 17.9σ . In addition we check that none of the modifications we do to the fit decreases this value significantly.

Finally putting all information together we obtain the ratio of branching fractions

$$R = \frac{\mathcal{B}(B_s^0 \rightarrow J/\psi f_0(980)) \mathcal{B}(f_0(980) \rightarrow \pi^+ \pi^-)}{\mathcal{B}(B_s^0 \rightarrow J/\psi \phi) \mathcal{B}(\phi \rightarrow K^+ K^-)} = 0.292 \pm 0.020 \pm 0.017. \quad (6)$$

Using the world average values for ϕ and $B_s^0 \rightarrow J/\psi \phi$ branching fractions we obtain

$$\mathcal{B}(B_s^0 \rightarrow J/\psi f_0(980)) \mathcal{B}(f_0(980) \rightarrow \pi^+ \pi^-) = (1.85 \pm 0.13 \pm 0.11 \pm 0.57) \cdot 10^{-4}, \quad (7)$$

where the first uncertainty is statistical, the second is systematic and the third one is due to the uncertainty on branching fractions. We do not calculate separate branching fraction of the pure $B_s^0 \rightarrow J/\psi f_0(980)$ decay due to the

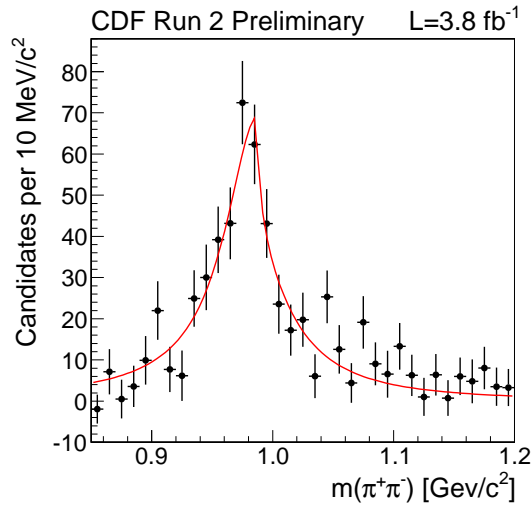


FIG. 5. The dipion invariant mass distribution after sideband subtraction with fit projection overlayed. Fit uses Flatté distribution with all parameters floating.

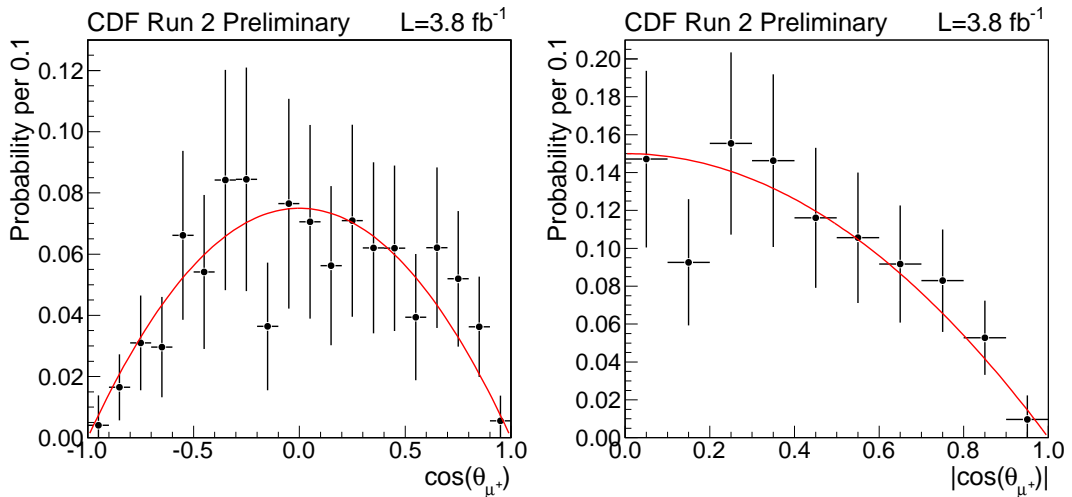


FIG. 6. The helicity angle distribution for positive muon corrected for relative efficiency. The line shows expectation for $B_s^0 \rightarrow J/\psi f_0(980)$ decay.

poorly known $f_0(980)$ branching fractions. The value of R is consistent with LHCb measurement [14] as well as with expectations which are in the range of 0.1 - 0.5.

ACKNOWLEDGMENTS

We thank the Fermilab staff and the technical staffs of the participating institutions for their vital contributions. This work was supported by the U.S. Department of Energy and National Science Foundation; the Italian Istituto Nazionale di Fisica Nucleare; the Ministry of Education, Culture, Sports, Science and Technology of Japan; the Natural Sciences and Engineering Research Council of Canada; the National Science Council of the Republic of China; the Swiss National Science Foundation; the A.P. Sloan Foundation; the Bundesministerium für Bildung und Forschung, Germany; the Korean World Class University Program, the National Research Foundation of Korea; the Science and Technology Facilities Council and the Royal Society, UK; the Institut National de Physique Nucleaire et Physique des Particules/CNRS; the Russian Foundation for Basic Research; the Ministerio de Ciencia e Innovación,

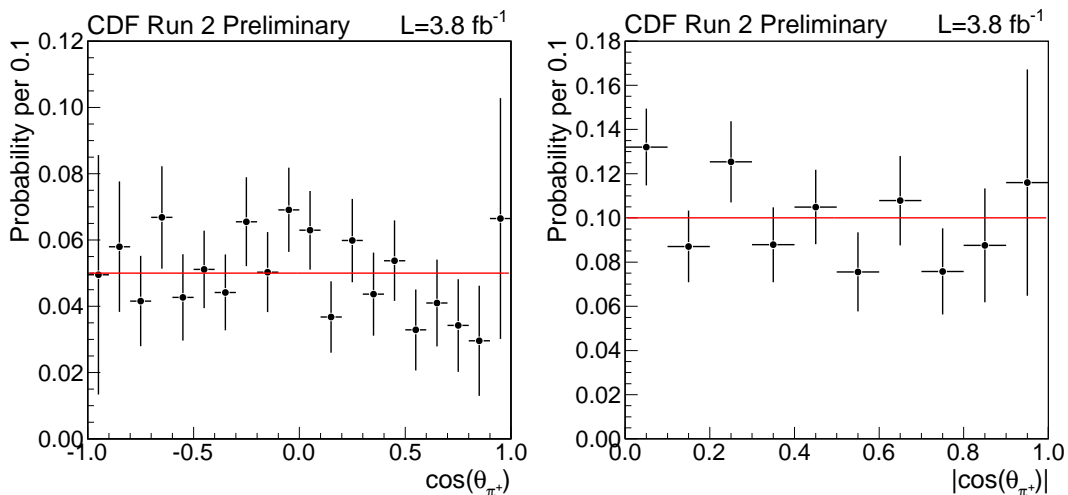


FIG. 7. The helicity angle distribution for positive pion corrected for relative efficiency. The line shows expectation for $B_s^0 \rightarrow J/\psi f_0(980)$ decay.

and Programa Consolider-Ingenio 2010, Spain; the Slovak R&D Agency; and the Academy of Finland.

-
- [1] A. Abulencia *et al.* (CDF Collaboration), Phys. Rev. Lett. **97**, 242003 (2006), arXiv:hep-ex/0609040.
[2] T. Aaltonen *et al.* (CDF Collaboration), Phys. Rev. Lett. **100**, 161802 (2008), arXiv:0712.2397 [hep-ex].
[3] V. M. Abazov *et al.*, Phys. Rev. Lett. **101**, 241801 (2008), arXiv:0802.2255 [hep-ex].
[4] T. Aaltonen *et al.* (CDF Collaboration), CDF Public Note 9458 (2008).
[5] S. Stone and L. Zhang, Phys. Rev. D , 074024 (2009), arXiv:0812.2832 [hep-ph].
[6] S. Stone, arXiv:1009.4939 [hep-ph].
[7] S. Stone and L. Zhang, arXiv:0909.5442 [hep-ex].
[8] K. Ecklund *et al.* (CLEO Collaboration), Phys. Rev. **D80**, 052009 (2009), arXiv:0907.3201 [hep-ex].
[9] P. Colangelo, F. De Fazio, and W. Wang, Phys. Rev. **D81**, 074001 (2010), arXiv:1002.2880 [hep-ph].
[10] P. Colangelo, F. De Fazio, and W. Wang, arXiv:1009.4612 [hep-ph].
[11] P. Colangelo, F. De Fazio, P. Santorelli, and E. Scrimieri, Phys. Rev. **D53**, 3672 (1996), arXiv:hep-ph/9510403.
[12] P. Ball and R. Zwicky, Phys. Rev. **D71**, 014029 (2005), arXiv:hep-ph/0412079 [hep-ph].
[13] R. Louvot (On behalf of the Belle collaboration), PoS **FPCP2010**, 015 (2010), arXiv:1009.2605 [hep-ex].
[14] R. Aaij *et al.* (The LHCb), arXiv:1102.0206 [hep-ex].
[15] J. Li *et al.* (Belle Collaboration), arXiv:1102.2759 [hep-ex].
[16] D. E. Acosta *et al.* (CDF Collaboration), Phys. Rev. **D71**, 032001 (2005), arXiv:hep-ex/0412071 [hep-ex].
[17] C. S. Hill (On behalf of the CDF Collaboration), Nucl. Instrum. Meth. **A530**, 1 (2004).
[18] A. A. Affolder *et al.* (CDF Collaboration), Nucl. Instrum. Meth. **A526**, 249 (2004).
[19] G. Ascoli, L. Holloway, I. Karliner, U. Kruse, R. Sard, *et al.*, Nucl. Instrum. Meth. **A268**, 33 (1988).
[20] E. J. Thomson, C. Ciobanu, J. Chung, J. Gerstenschlager, J. Hoftiezer, *et al.*, IEEE Trans. Nucl. Sci. **49**, 1063 (2002).
[21] M. Feindt and U. Kerzel, Nucl. Instrum. Meth. **A559**, 190 (2006).
[22] M. Feindt, arXiv:physics/0402093.
[23] D. Lange, Nucl. Instrum. Meth. **A462**, 152 (2001).
[24] R. Brun, R. Hagelberg, M. Hansroul, and J. Lassalle, (1978), cERN-DD-78-2-REV.
[25] E. Gerchtein and M. Paulini, ECONF C0303241 , TUMT005 (2003), arXiv:physics/0306031 [physics].
[26] G. Punzi, PHYSTAT-2003 , MODT002 (2003), arXiv:physics/0308063.
[27] K. Nakamura *et al.* (Particle Data Group), J. Phys. **G37**, 075021 (2010).
[28] F. Abe *et al.* (CDF Collaboration), Phys. Rev. **D54**, 6596 (1996), arXiv:hep-ex/9607003.
[29] T. Aaltonen *et al.* (CDF Collaboration), CDF Public Note 10206.
[30] M. Gronau and J. L. Rosner, Phys.Lett. **B669**, 321 (2008), arXiv:0808.3761 [hep-ph].
[31] S. M. Flatte, Phys. Lett. **B63**, 224 (1976).
[32] M. Ablikim *et al.* (BES Collaboration), Phys. Lett. **B607**, 243 (2005), arXiv:hep-ex/0411001.